ELSEVIER

Thermochimica Acta 357–358 (2000) 267–278

thermochimica acta

www.elsevier.com/locate/tca

Determination of heat capacity with a sawtooth-type, power-compensated temperature-modulated DSC☆

R. Androsch[a,b,*], I. Moon[a,b], S. Kreitmeier[c], B. Wunderlich[a,b]

[a]*Department of Chemistry, The University of Tennessee, Knoxville, TN 37996-1600, USA*
[b]*Oak Ridge National Laboratory, Chemical and Analytical Sciences Division, Oak Ridge, TN 37831-6197, USA*
[c]*Institut für Experimentelle und Angewandte Physik, Universität Regensburg, Regensburg, D-93040, Germany*

Received 9 November 1998; accepted 28 January 1999

Abstract

The determination of the heat capacity in sawtooth-type, power-compensated temperature-modulated differential scanning calorimetry (TMDSC) by evaluation of the first harmonic of the Fourier transformation of the sample temperature and heat-flow rate is analyzed with experiments and model calculations. At modulation periods below 100 s, the measured, uncorrected, absolute value of the complex heat capacity deviates exponentially from the true heat capacity, while the steady state within the linear heating and cooling segments is reached after about 50 s. The errors increase with the heat capacity of the sample and vary for different samples and configurations of the measurement. An empirical equation for correction is suggested. It uses a sample-mass and instrument-dependent time constant $\tau(m)$ and permits measurements down to periods of 15 s, i.e., much before steady state is reached within the linear segments of the modulation experiment. © 2000 Published by Elsevier Science B.V.

Keywords: DSC; TMDSC; Sawtooth-modulation; Fourier transformation; Heat capacity

1. Introduction

The experimental determination of heat capacity with standard differential scanning calorimetry (DSC) is a well-established method with an accuracy which routinely reaches approximately 3% [1]. The measurement includes an optimization of sample mass, heating rate, baseline-linearity and the heat-conduction path between temperature sensor, pan, and the well-packed sample [2,3]. The recently introduced temperature-modulated DSC (TMDSC) using the heat-flux principle is considered to produce even more accurate heat capacities since irreversible effects, such as instrumental heat losses and irreversible structural changes in the sample, present in the standard DSC heat-flow rate, can be separated by analyzing only the heat-flow response to the given modulation frequency [4–6]. Furthermore, the heat capacity can be determined quasi-isothermally with experiments that extend over a sufficient period of time to guarantee steady state [4].

* Corresponding author. Tel.: +1-423-574-4989; fax: +1-423-576-5235.

0040-6031/00/$ – see front matter © 2000 Published by Elsevier Science B.V.
PII: S0040-6031(00)00397-X

In TMDSC, a periodic temperature change is superimposed on the constant heating rate $\langle q \rangle$, typical for the standard DSC. The modulation of the temperature is usually a continuous, sinusoidal oscillation or composed of linear heating and cooling segments, a so-called sawtooth. The periodic component of the sample temperature is described by its amplitude A_{TS} in kelvin and frequency ω in radians per second ($=2\pi/p$, where p is the period in s). The corresponding heat-flow rate into the sample, HF, is the response to the linear heating rate and the temperature modulation, and must be deconvoluted for analysis.

The underlying, constant heating rate $\langle q \rangle$ is extracted from the superposition of constant and oscillating rates by averaging the time-dependent rate $q(t)=dT/dt$ over one modulation period of $t \pm p/2$. This sliding average with t is indicated by the angular brackets $\langle\ \rangle$. Similarly, the total heat-flow rate due to the constant heating-rate component is given by $\langle HF \rangle$. The total heat capacity of the sample can then under the assumption of steady state be calculated in analogy to the standard, not-modulated DSC as [2]:

$$(C_s - C_r) \approx \frac{\langle HF \rangle}{\langle q \rangle} \tag{1}$$

where C_s, represents the heat capacity of the sample calorimeter (sample+pan) and C_r, is the heat capacity of the reference calorimeter (usually an empty pan). A minor correction, needed to account for differences in heating rates between sample and reference calorimeters were derived for the heat-flux calorimeter as $+(C_s + C_r) \times (d\Delta T/dT_r)/[1 - (d\Delta T/dT_r)]$, where $\Delta T = T_r - T_s$ [2]. Although easily computed, this correction is rarely applied, although it may cause an error of 1–3% in a well-adjusted DSC and more otherwise. For power-compensated DSC such corrections have never been studied, but may in the light of the present work be worth considering for increases in precision beyond ±1%.

The modulation, in turn, causes a reversing heat-flow rate response. It is commonly represented by the amplitude of the first harmonic of the Fourier representation of the heat-flow rate, A_{HF}:

$$HF(t) = \langle HF \rangle + \sum_{v=1}^{\infty} [A_v \sin(v\omega t) + B_v \cos(v\omega t)] \tag{2}$$

where A_v and B_v, are coefficients that must be determined in the usual manner, and v is an integer. An analogous equation has to be used for the sample temperature. As long as the modulation starts at $t=0$ and is symmetric about $\langle q \rangle t$, the modulation is centrosymmetric and all B_v, are zero, i.e., the series contains only the sinusoidal harmonics. For a linear response of the sample to a sinusoidal modulation, no higher harmonics are generated in the heat-flow rate, i.e., $A_{HF} = A_{HF1}$. A centrosymmetric sawtooth modulation also simplifies the Fourier representation, it shows only odd, sinusoidal harmonics with $v=1, 3, 5$, etc.

In case the first harmonics do not represent the modulated parameter fully, it is necessary to use the full expression of Eq. (2). Small differences were found during the glass transition [6–8]. The slow response of samples in the glass transition region causes (1) higher harmonics due to the co-operative freezing or unfreezing of large-amplitude motion, (2) frequency shifts due to coupling of the linear and modulated time scales, and (3) an asymmetry in the reversing response due to the exponential temperature dependence of the relaxation times. Larger differences in the description of the modulated parameter can show up in first-order transitions. The observed problems are as follows: (1) the transitions may be fully or partially reversible or even completely irreversible. (2) Large exotherms or endotherms may cause time periods of constant temperature within the sample, followed by renewed approaches to the prior steady state. (3) Steady state may be lost over more than one modulation period. (4) Irreversible processes may contain accidental Fourier components of the modulation frequency. (5) The transition kinetics may cause lags in the sample response. For a recent summary of theses effects see [9]. In any of these cases it is necessary to inspect the heat-flow rate in the time domain, $HF(t)$, before accepting 'apparent heat capacities' computed from a first-harmonic Fourier fit of the reversing parameters.

For heat-flux calorimeters the following equation was derived for the reversing heat capacity (the absolute value of the complex heat capacity) [5]:

$$(C_s - C_r) = \frac{A_{HF}}{A_{TS}\,\omega} \sqrt{1 + \left(\frac{C_r}{K}\right)^2 \omega^2} \tag{3}$$

where A_{HF} and A_{TS} are the amplitudes of the first harmonic of the corresponding Fourier series of Eq. (2) (v=1). A difference between the results of Eqs. (1) and (3), if it exists, represents the nonreversing heat-flow rate, i.e., the part of the heat-flow rate which does not follow the modulation [10,11]. Outside of the glass-transition and melting regions, the heat capacities of liquids and solids follow the modulation instantaneously because the heat-flow rate responds sufficiently fast to changes in temperature. In this case, measurements are limited only by the thermal conductivity. Typical response times of molecular motions are in the picosecond range (10^{-12} s) [2,12], much shorter than the applied period of oscillation of the temperature, which may lie between 10^1 and 10^3 s. Thus, the heat capacity produces almost always a reversing heat-flow rate and, in absence of irreversible processes, the nonreversing part of the heat-flow rate is zero. In case the modulation is performed quasi-isothermally ($\langle q \rangle$=0), the total heat-flow rate $\langle HF \rangle$ should also be zero for samples which behave reversibly on heating and cooling. If this is not so, any remaining nonreversing heat-flow rate must be discussed in terms of an irreversible sample behavior, instrument losses and instabilities, or both. Irreversible changes due to the sample response to the modulation can be eliminated in quasi-isothermal experiments by extending the time before data collection until the irreversible process is completed.

In this paper, quasi-isothermal measurements using sawtooth-modulation with a power-compensated TMDSC are analyzed to test the applicability of this method to heat capacity measurements and to elucidate the differences to temperature-modulated heat-flux calorimetry. In a parallel investigation of the heat-flux DSC 820 of Mettler-Toledo, it was found that heat capacities measured by sawtooth-type TMDSC show also a distinct dependence on frequency [13]. This was attributed to the thermal conductivity of the sample. If the shift in the phase between sample temperature and its corresponding heat-flow rate is known, this dependence on frequency can be corrected. Similar results are obtained in finite-element calculations applied to heat-flux and powercompensating instruments [14]. Furthermore, model calculations have shown that from the point of view of the Fourier analysis of a heat-flux calorimeter, heat capacities can be determined even if steady state is not reached, as long as both, the temperature and temperature-difference response is to the same furnace [9,15].

For the power-compensating type of DSC, the sample properties seem to be of greater importance due to the different instrument design [16,17]. Again, if the phase-shift between the heating rate of the sample and the heat-flow rate is available, corrections can be made [17]. Naturally, it is of interest to find out to what degree equivalent statements can be made for power-compensation calorimetry which has a different heat-flow path then is used in heat-flux calorimetry. It is of importance to keep in mind that the principle of the heat-flux DSC is to achieve a negligible temperature gradient between the sample and sample-temperature sensor relative to the temperature gradient which is set up between the heater and sample-temperature sensor [2]. The latter temperature gradient is used, when compared to the temperature gradient from the same heater to the reference calorimeter, to estimate the heat-flux rate. The power-compensation DSC, in contrast, has its separate heaters for sample and reference calorimeters in close proximity to the respective temperature sensors. The differential power generated and measured as heat-flux rate is programmed to yield a negligible temperature difference between sample sensor and reference sensor [2]. This makes the temperature gradients between the sample-temperature sensor and the sample and the reference -temperature sensor and the reference a major concern for the performance of the instrument. In this paper, experimental results are presented that lead to the correction equation for the evaluation of heat capacities over wider modulation-frequency ranges and result in a better understanding of the temperature-modulated power-compensation DSC.

2. Experimental

Heat capacity measurements were performed with a Perkin–Elmer DSC 7 with an intracooler as cooling accessory and the 7 Series/Unix software package for data collection. The temperature and energy calibration of the instrument was performed using the onset melting temperatures of indium and tin, and the heat of fusion of indium, respectively. The additional,

customary point by point calibration of the heat-flow rate with sapphire (Al_2O_3) was not undertaken, for reasons that will become obvious in the body of this paper. Additionally, the furnace temperature was calibrated to match the program and sensor temperatures. The furnace was purged with nitrogen at a flow rate of 20 ml min^{-1}. The quasi-isothermal modulation temperature for all experiments was chosen to be 298.15 K. The sawtooth amplitude and period were varied. The software requires the input of a baseline run obtained using the same conditions (pan type and mass) as in the sample run, but without the sample. The heat-flow rate of this baseline run is subtracted from the sample run in the time-domain, correcting for any asymmetry of the differential calorimeter. Furthermore, a dynamic *K*-factor, available in the Perkin–Elmer Software [18] for correction of errors due to insufficient equilibration times, was set to one in each experiment, i.e., it was not applied to the data. The experimental data, consisting of heat-flow rate and sample temperature, were recorded versus time after correction for the baseline, and saved as ASCII data for external processing. This was necessary since the available software version of the instrument performs an over-correction of the phase lag which affects the calculation of the heat capacity [19]. Furthermore, the phase lag, necessary for corrections as suggested in [17], was not available in its uncorrected form. The available, corrected tan δ was naturally always zero in the quasi-isothermally performed heat capacity measurements. Materials used in this investigation were aluminum, sapphire (Al_2O_3), and atactic polystyrene.

3. Results

Fig. 1 shows the heat capacity of polystyrene (sample mass 11.93 mg) at 298.15 K as a function of the modulation period. The open symbols represent data calculated using the amplitudes of the first harmonic of the Fourier fit of the heat-flow rate and the sample temperature to an equation similar to Eq. (3), thought to represent the reversing heat-flow rate of the power-compensated DSC:

$$mc_p = \frac{A_{HF}}{A_{TS}\,\omega}\,K' \qquad (4)$$

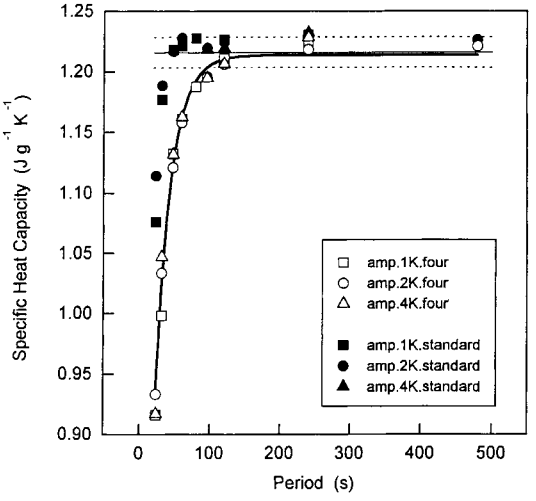

Fig. 1. Specific heat capacity of polystyrene as function of the modulation period and amplitude, calculated using the standard DSC equation, Eq. (1), and the Fourier fit for Eq. (4).

where K' is a dimensionless calibration constant which is set to one in all calculations, if not stated otherwise. Note the similarity of Eq. (4) to Eqs. (1) and (3).

The filled symbols were calculated using the equation for the standard DSC [Eq. (1)]. Data were taken in the temperature region where steady state was most closely approached for the given conditions, i.e., at the time just before switching the sign of the heating rate or over the range of time of obvious steady state. The thin solid line is the expected heat capacity, as listed in the ATHAS data bank [20]; the dotted lines mark the $\pm 1\%$ error range. The bold line is an arbitrary fit to the open symbols, made to show the difference between the two calculation methods. The modulation amplitudes of 1, 2, and 4 K were realized by choosing different heating and cooling rates. The modulation amplitude seems to have no influence on the frequency dependence. The heat capacities calculated by both methods get progressively smaller when the period is decreased. The most striking difference between the two calculations is the initial period when larger deviations of the calculated from the true value occur. In the case of the Fourier fit, the deviation from the true heat capacity starts at a period of $\approx$96 s. In the case of standard DSC, this critical value is shifted to $\approx$48 s.

Fig. 2 contains similar data for sapphire (sample mass 22.14 mg). The standard DSC equation gives

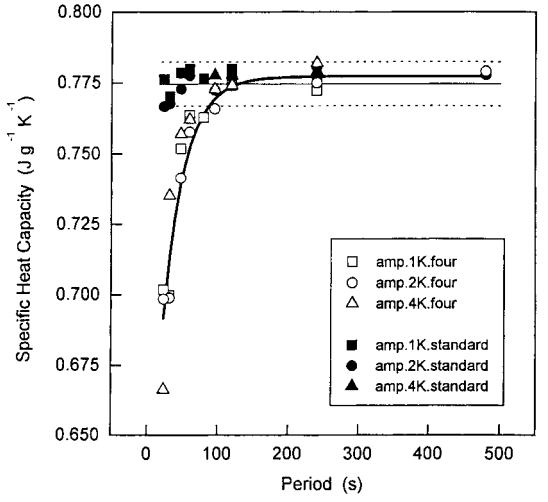

Fig. 2. Specific heat capacity of sapphire as function of the modulation period and amplitude, calculated using the standard DSC equation, Eq. (1), and the Fourier fit for Eq. (4).

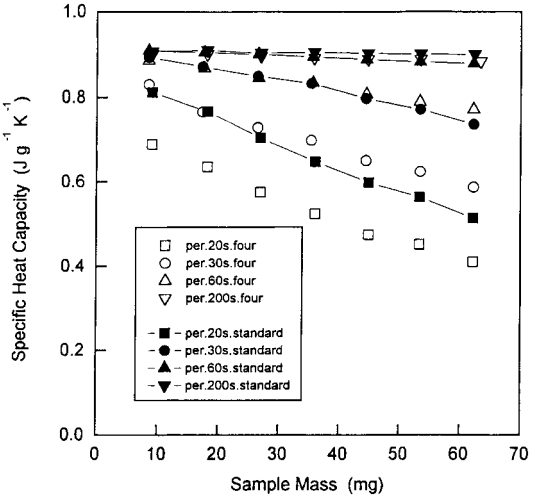

Fig. 3. Specific heat capacity of aluminum as function of the sample mass and modulation period, calculated using the standard DSC equation, Eq. (1), and the Fourier fit for Eq. (4).

correct data for practically all periods analyzed (24–480 s), whereas the Fourier fit results in a similar dependency of the heat capacity on the modulation period as shown in Fig. 1 for polystyrene. The differences must be attributed to the individual thermal conductivities α of those samples — α(PS)/α(Al)$\approx$0.02; $\alpha(Al_2O_3)/\alpha$(Al)$\approx$0.86 [21]. The modulation amplitude does not show a trend of the calculated heat capacities, as is also seen in the case of polystyrene.

The influence of the sample mass on the calculated heat capacity was analyzed for Al as an additional parameter to the modulation period and amplitude. The data are shown in Fig. 3. An increasing sample mass, as well as a shorter modulation period reduces the measured heat capacity. Again, the Fourier fit results in larger deviations from the expected value when compared to the heat capacity calculated by the standard DSC equation. The different sample masses in the experiment were realized by stacking different numbers of aluminum lids with masses of $\approx$9 mg each into the sample pan.

In Fig. 4 the heat capacity of aluminum is plotted as measured in different experimental configurations. The first two experiments used no pans and had samples of one and two aluminum lids (■ and □, respectively, the baseline runs for these experiments were carried out with empty reference and sample calorimeters). Next, a sample of two aluminum lids was placed into an open aluminum pan of=17 mg (◆, the baseline run for this experiment consisted of an empty reference calorimeter and a sample calorimeter with an empty pan). Finally, the sample of two aluminum lids was placed into an open pan that contained one additional lid (◇, the baseline run for this experiment consisted of an empty reference

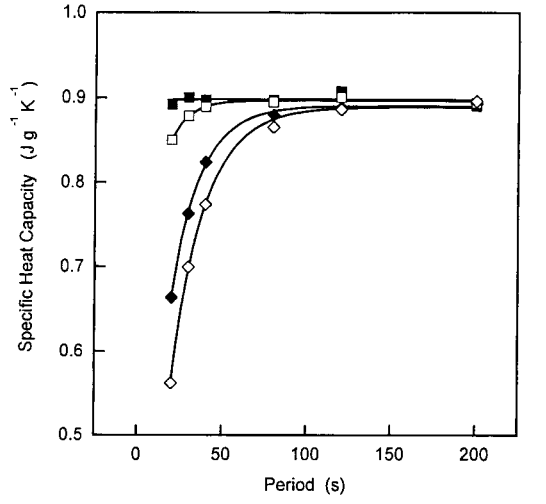

Fig. 4. Specific heat capacity of aluminum as function of the modulation period for four different experimental set-ups, calculated using the Fourier fit for Eq. (4).

calorimeter and a sample calorimeter with a pan filled with one lid).

Additional measurements with different heat capacities in the reference calorimeter result in the same type of data [22]. The shown data are selected from a larger number of experiments which all demonstrate an influence of the path length on the heat-flow rate. All data are calculated with Eq. (4) via the Fourier fit. It becomes clear that the heat-transfer conditions systematically alter the point where the heat capacity deviates first from its true value. As the path length and the absolute heat capacity of the sample increase, the first deviation occurs at a larger period.

4. Discussion

4.1. Standard DSC equation

When analyzed with the standard DSC method, as illustrated in Fig. 1, the period of measurement of the heat capacity of polystyrene must be longer than 48 s for the chosen conditions. The cause of failure at smaller p is due to the inability to reach steady state before the next segment of modulation starts. This well-known prerequisite of steady state for the measurement by a standard heat-flux DSC can be seen from the integration of the heat-flow-rate equation for a heat-flux DSC [2]:

$$\frac{dQ}{dt} = K\left[\langle q\rangle t - \frac{Q}{C_p}\right] \quad (5)$$

$$Q = \langle q\rangle C_p\left[t - \frac{C_p}{K}(1 - e^{-Kt/C_p})\right] \quad (6)$$

where dQ/dt is the heat-flow rate into a single calorimeter. For not to large modulation amplitudes, Eq. (6) describes also the change of the temperature of the calorimeter via $Q=C_p\,(T-T_0)$. Only at a sufficiently extended half-period ($p/2$) does the measured heat capacity of Eq. (1) reach a constant value before switching to the next segment [i.e., $\exp(-Kt/C_p)=0$, where t is counted from the prior switch in the heating rate of the sawtooth]. Calibration materials like sapphire cannot be used to correct the non-steady-state heat-flow rate. The sapphire runs shown in Fig. 2 were collected under the same conditions as the polystyrene runs but they can not be used for correction of the polystyrene data when $p<48$ s, as is illustrated in Fig. 5. For measurement of the heat capacity by standard DSC without modulation, it is naturally always possible to extend the heating or cooling periods to finally reach steady state. The ultimate limit for a quality heat-capacity measurement is the generation of an excessive temperature gradient within the sample. Typically, this limit is reached for small sample masses at a $\langle q\rangle$ of about 40 K min^{-1}, and the temperature range that can be covered with one run is 50–100 K in the absence of transitions [2].

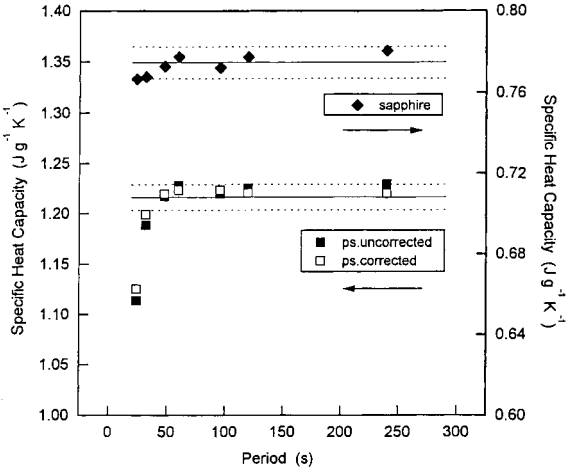

Fig. 5. Attempt to correct the polystyrene data of Fig. 1 (modulation amplitude 2 K) with the sapphire data of Fig. 2 using the standard DSC equation, Eq. (1).

4.2. Fourier description of the amplitudes of modulated temperature and heat-flow rate

The application of Eq. (4) to the calculation of the heat capacity requires that the amplitudes of the heat-flow rate, A_{HF} (proportional to $T_r-T_s=\Delta T$), and the heating rate, $A_{TS}\omega$, of the first harmonic of the appropriate Fourier series have the same fractional deviations from the steady state values of Eq. (1). Only then can Eqs. (4) and (1) give the same results. For a quasi-isothermal experiment ($\langle q\rangle=0$), the heat-flow-rate equation and its solution can be written in analogy to Eqs. (5) and (6). The new equations were derived for a sinusoidal modulation [5,6], but can easily be extended to the Fourier series of a

centrosymmetric sawtooth:

$$\frac{dQ}{dt} = K\sum_{v=1}^{\infty}[A_v \sin(v\omega t)] - \frac{KQ}{C_p} \quad (7)$$

$$Q = \sum_{v=1}^{\infty} \frac{KA_v}{(K/C_p)^2 + v^2\omega^2} \times \left[\left(\frac{K}{C_p}\right)\sin v\omega t - v\omega \cos v\omega t + v\omega e^{-Kt/C_p}\right] \quad (8)$$

Eq. (8) can also be expressed in terms of temperature, as pointed out above, and by introducing the phase shift ε_v, from $\tan \varepsilon_v = v\,\omega\, C_p/K$, the temperature of the calorimeter becomes:

$$T = \sum_{v=1}^{\infty} A_v[\sin(v\omega t - \varepsilon_v) + \sin \varepsilon_v\, e^{-Kt/C_p}] \quad (9)$$

Each of the independent terms of the solution of the linear, first-order differential equation, Eq. (7), yields the proper value for the reversing heat capacity when inserted as $A_{HF}(v)/[A_{TS}(v)\omega(v)]$ into Eq. (3). The obvious choice for the analysis is the first harmonic since it has the largest amplitude.

Next, it could be shown by model calculations that for a DSC of the heat-flux type it is not even necessary that the linear segments of the sawtooth reach steady state before Eq. (3) holds [9,15]. A remaining stringent condition is, however, that the temperature gradient within the sample continues to be negligible.

Fig. 6A and B illustrate the fit of two of the polystyrene data sets. One that was analyzed under steady-state conditions (period 480 s) and the other, far from steady state (period 24 s). The upper curves of Fig. 7 represent the deviations encountered in representing the true amplitudes of the heat-flow rate (A_{HF}, ■) and the heating rate ($A_{TS}\,\omega$, □) by the first harmonic of the Fourier series; the corresponding triangles (▲, △) are the sapphire data. The lower curves give the ratios of the corresponding two sets of upper curves. If the deviations were compensating, the ratios should be 1.0. The change of this ratio is different for polystyrene (◆) and sapphire (◇) so that the sapphire data cannot be used for correction of the polystyrene data. The ratio of the fitted and true heating-rate amplitudes is the same for polystyrene (□) and sapphire (Δ). This is a characteristic of the power-compensation calorimeter which produces an almost sample-independent sensor-temperature amplitude [23].

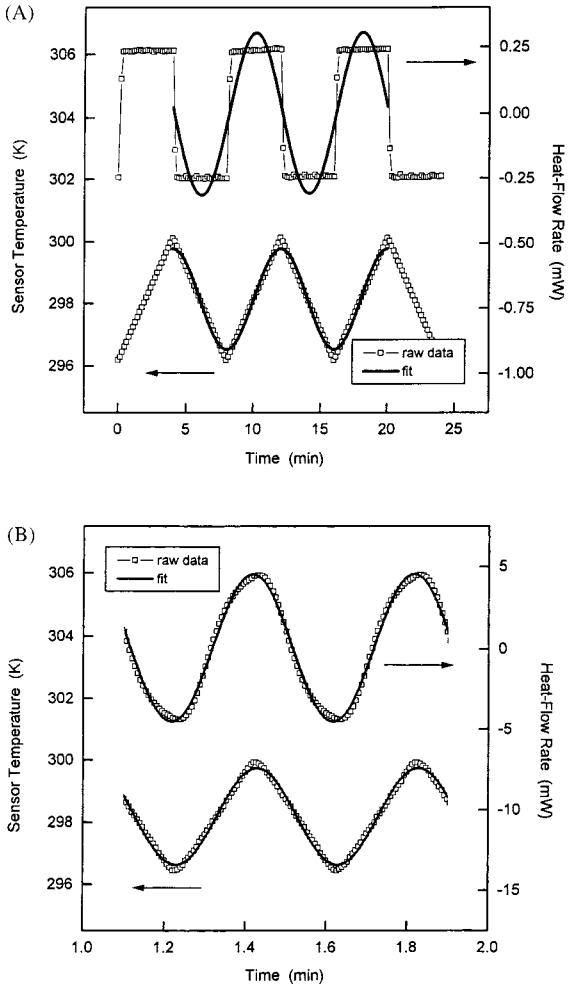

Fig. 6. Quasi-isothermal measurement on polystyrene at 298.15 K with a modulation amplitude of 2 K, (A) period p=480 s and (B) period p=24 s.

4.2.1. Performance characteristics of power-compensation and heat-flux calorimeters

The heat-flux DSC uses one common heater for both, the sample and the reference. The temperature sensors are located in close proximity of the sample and reference, respectively, to assure a negligible temperature gradient. Therefore, the heat conduction path from the heater to the sample and reference is much longer than that from the sample and reference

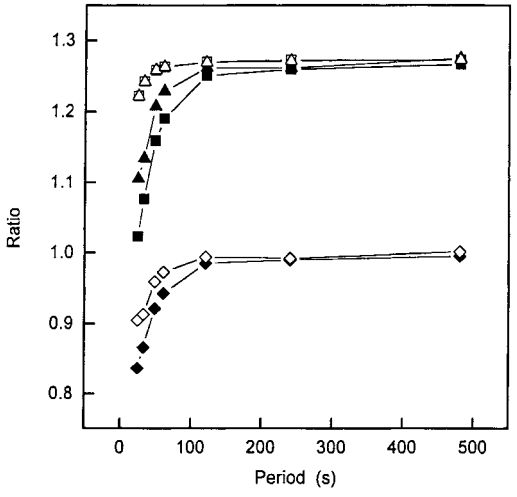

Fig. 7. Upper curves: ratios between fitted and true amplitudes of heat-flow rates and heating rates. Lower curves: ratios between fitted amplitudes of heat-flow rates and heating rates of polystyrene and sapphire data from Figs. 1 and 2.

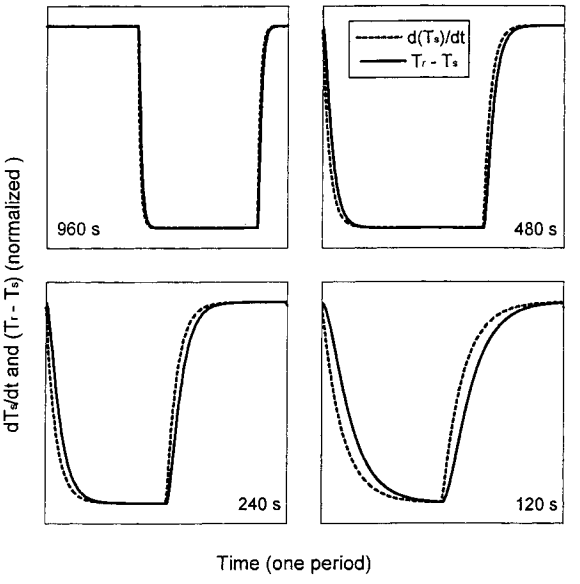

Fig. 8. Simulation of the time-dependency of the heating rate (dT_s/dt) and the difference between reference and sample temperature ($T_r - T_s$) for different periods p.

to the sensors. The difference between the larger temperature gradients from the heater to the sample and reference sensors is the measure of the sample heat flux. The power-compensation DSC [24,25] has a much shorter total path for heat conduction from the individual heaters to the sample and reference and their corresponding sensors. The electronics controls the average temperature according to the temperature program and compensates almost any temperature difference between the sensors of the isolated sample and reference calorimeters. A small, usually negligible, temperature difference remains and is directly proportional to the recorded differential power. The differential power needed to minimize this temperature difference is proportional to the sample heat flux. Larger temperature differences develop when the sample suffers a large first-order transition over a narrow temperature range, a case that needs to be treated separately, perhaps in analogy to the discussion completed for heat-flux calorimetry [9,15], but is outside the frame of the present investigation. The delay in reaching steady state of the heat-flow rate and heating rate comes from the need to transfer the heat from the reference and sample heaters into the reference and sample calorimeters. This process is similar to the heat-flow rate from heater to the sample-temperature sensor which governs the heat-flux DSC. One may, thus, assume that an equation similar in form to Eq. (3) that was derived for heat-flux DSC [5] can be used to correct the heat-flow rate of the power-compensation DSC.

A modeling experiment was undertaken to explore the effects of the different delays in reaching steady state of the heating rate dT_s/dt, and the difference between sample and reference temperatures ($T_r - T_s$, proportional to the heat-flow rate) on the heat capacity measurement. The approach is similar to earlier calculations that apply to the heat-flux calorimetry [9,15]. In Fig. 8 we show the results for one period after repeatable modulation has been reached (third cycle). The heating rate and the heat-flow rate were both normalized to the maximum amplitude. Visual inspection of the data clearly explains the differences in the heating rate and heat-flow rate amplitudes expected from the fit to a Fourier series. A quantitative evaluation of the differences between the fitted and the true values is shown in Fig. 9. The results are comparable to the experimental data of Fig. 7. The heat capacity when determined by the Fourier fit via Eq. (4) must, thus, also be dependent on the frequency of the measurement as long as no corrections are applied to compensate for the different approaches to steady

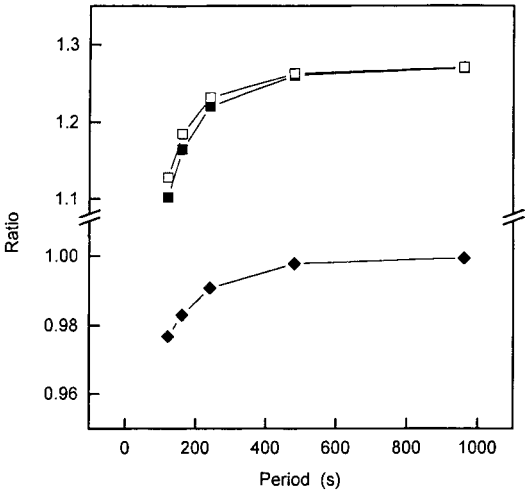

Fig. 9. Upper curves: ratios between Fourier fitted (TMDSC) and true (DSC) amplitudes of heat-flow rates (■) and heating rates (□). Lower curve: ratios between Fourier fitted amplitudes of heat-flow rates and heating rates based on the simulation data in Fig. 8 (◆).

state of the heating rate and the heat-flow rate. This holds regardless whether the system is in steady state for each linear segment of the sawtooth (as in standard DSC), or not, as is displayed in Fig. 10. Application of Eq. (1) of the standard DSC gives the correct value for C_p/K (=10−5 s) as long as the calorimeter reaches

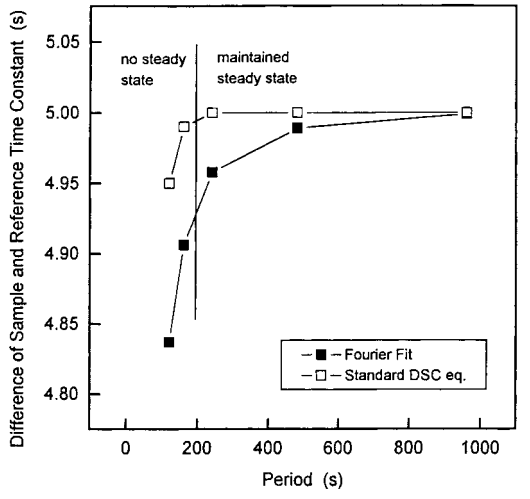

Fig. 10. Difference of sample and reference time constants as function of the period as calculated from the simulated data shown in Fig. 8.

steady state at the switch of heating rate. A calculation via Fourier fit, in contrast, contains already a non-negligible error when assessed with Eq. (4). Since the absolute heat capacity in $J\,K^{-1}$ changes the time constant of the equilibration into steady state, the experimental data shown in Fig. 3 can now be explained: the experiment shows no dependence of the sample-temperature amplitude on the sample mass, but steady state is approached more slowly with increasing mass (heat capacity of the calorimeter), resulting in a reduced amplitude of the first harmonic of the Fourier fit. Similarly, if the Newton's-law constant K is increased, as for instance by extending the path length between sensor and sample as realized in Fig. 4, it must affect the heat capacity calculated by the Fourier-fitted amplitudes.

4.3. Corrections for differences in approach to steady state for heating rate and heat-flow rate

In the discussion of the experimental data, the dimension-less heat-capacity calibration constant K' in Eq. (4) was set to one after a calibration of the instrument with the heat of fusion of indium. From the experience with heat-flux calorimetry one knows, however, that Eq. (4) needs to be corrected for the differences between the heat-flow rates into the reference and sample calorimeters. The corrected equation for the heat-flow case could be derived, according to the discussion in the prior section, as Eq. (3) [5]. It involves the frequency ω, Newton's law constant K [$J\,K^{-1}\,mol^{-1}\,s^{-1}$], and the reference heat capacity C_r. Comparison of Eqs. (3) and (4) leads for the case of identical sample and reference pans ($C_s=C_r+mc_p$) to the following correction factor for the heat capacity constant of Eq. (4):

$$K' = \sqrt{1 + \left(\frac{C_r\omega}{K}\right)^2} \tag{10}$$

Assuming, next, that the power-compensation calorimeter needs a similar correction, we attempted to extract from the present data an appropriate time constant $C/K=\tau$ which has a dimension of [$s\,rad^{-1}$]. For the case of the simulated data in Figs. 8–10 this correction is easy to perform since the heat capacity is given already in terms of τ, i.e., the value of K needs not to be known explicitly. The correction of the

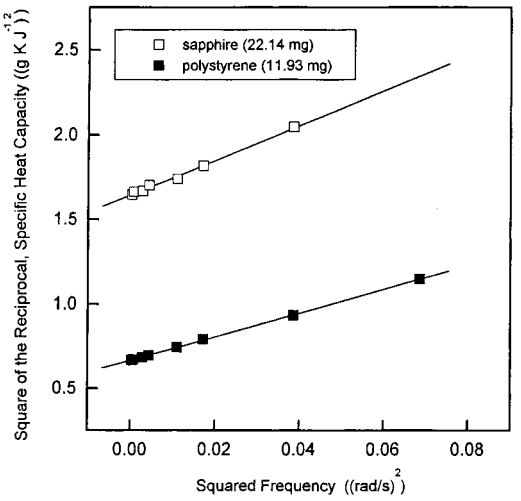

Fig. 11. Square of the reciprocal, uncorrected specific heat capacity of sapphire and polystyrene as function of the square of the modulation frequency ω, based on data of Figs. 1 and 2.

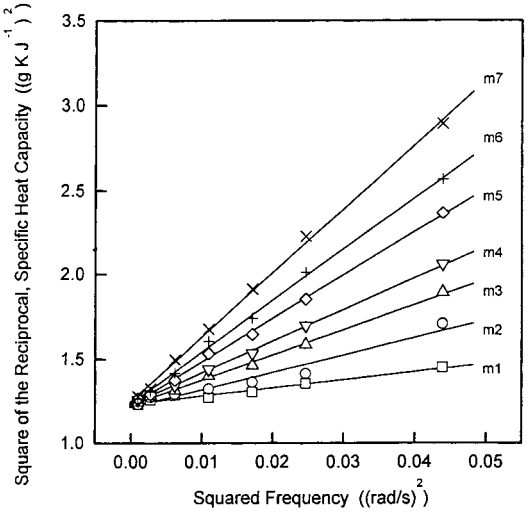

Fig. 12. Square of the reciprocal, uncorrected specific heat capacity of aluminum as function of the square of the modulation frequency ω, based on the data from samples of different mass as given in Fig. 3. Curves m_1 to m_7 refer to runs with 1–7 Al sample-pan lids, each of about 9 mg.

experimental data requires according to Eq. (10) a plotting of the square of the reciprocal of the uncorrected heat capacity versus the square of the frequency:

$$\frac{1}{C_p^2(\text{uncorrected})} = \frac{1}{C_p^2(\text{corrected})} \times [1 + (\omega\tau)^2] \tag{11}$$

The intercept of the fitted linear relation at $\omega^2=0$ is the inverse square of the corrected heat capacity, and from the slope, τ can be calculated. This is demonstrated in Fig. 11 for the polystyrene and sapphire data of Figs. 1 and 2, and in Fig. 12 for the aluminum data of different masses of Fig. 3. It can be seen that all data result in straight lines in support of the assumptions that went into Eq. (11). With the corrected K', all frequency dependence of the experimental data is eliminated as long as data of Figs. 11 and 12 remain linear. It needs to be pointed out, that this correction works also in the frequency range where steady state is not reached in the linear sawtooth segments, i.e., for the polystyrene data at periods shorter than 48 s. Furthermore, it is important to note that the slope changes with the material analyzed and also the sample mass.

From the experimental data in Figs. 11 and 12, one must conclude that indeed, the temperature gradients between the sample heater and actual sample temperature and the reference heater and the reference temperature are involved in the correction of K'. This result is in agreement with the descriptions of the heat-flux and power-compensation calorimeters given in the Section 1. When only one heater governs the differential heat flux, and the modulation is controlled at the sample with negligible temperature gradient between sample and sensor, only one correction is necessary, and takes the form of C_r/K i.e., the correction is sample-mass and material independent. In the power-compensation calorimeter the sample-dependent part of the time constant can be extracted by plotting the slope as defined in Eq. (10) versus the square of the sample mass and extrapolating to zero sample mass. This is done in Fig. 13 based on the aluminum data of Fig. 3. Collecting all the effects on the experimentally measured heat capacities into one equation, one obtains the following correction factor to be applied in Eq. (4):

$$K' = \sqrt{1 + [\tau(m)^2]\omega^2} \tag{12}$$

The experiments have shown that this equation holds up to a frequency of approximately $2\pi/15$ rad s^{-1}. This limit is in the same range, or even

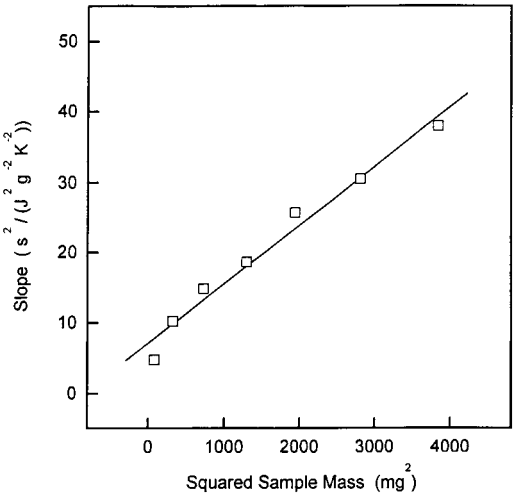

Fig. 13. Slope of Eq. (11) as a function of the square of the sample mass, based on data in Figs. 3 and 12.

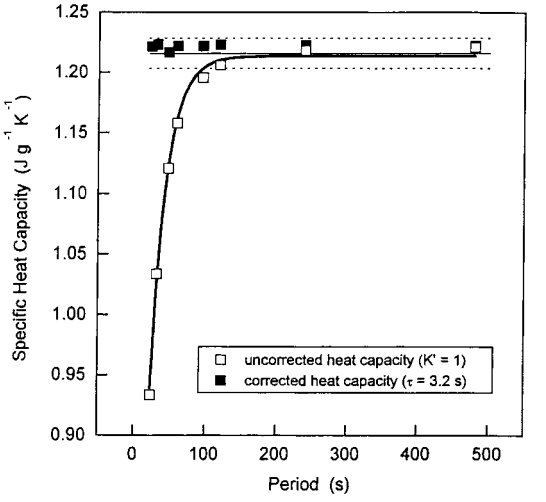

Fig. 15. Correction of the specific heat capacity of polystyrene according to Eqs. (4) and (12) with τ=3.2 s, based on data in Fig. 1.

better, than the limit observed in heat-flux instruments [26]. Since $\tau(m)$ is dependent on the type of the sample, a calibration with substances like sapphire is not valid. In Fig. 14 the consequence of such an improper correction of the polystyrene data of Fig. 1 (amplitude 2 K) with the corresponding sapphire data of Fig. 2 is displayed. It does not remove the frequency dependence of the measured specific heat capacity. Fortunately, the precise determination of the heat capacity does not require an explicit determination

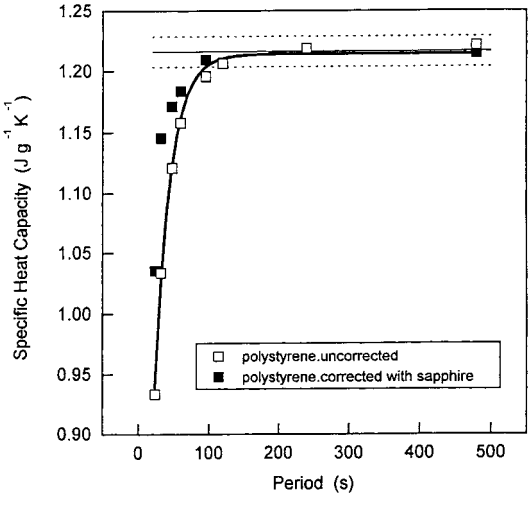

Fig. 14. Unsuccessful correction of the specific heat capacity of polystyrene with sapphire data, based on data in Figs. 1 and 2.

of K' and τ. It is possible to simply plot the reciprocal of the square of the measured value [Eq. (4) with K'=1] versus the square of the frequency ω^2 and extrapolate to zero. The intercept gives the reciprocal of the square of the correct heat capacity.

If data at a single frequency need to be corrected, the K' value must be known from a separate calibration for the given sample and reference, as described above. Each measured value can then be corrected, as is shown in Fig. 15. For the correction in Fig. 15 a $\tau(m)$ of approximately 3 s rad^{-1} was used.

Although it is not yet proven if the power-compensated DSC with sawtooth modulation produces more accurate heat capacities than the standard power-compensated DSC, the advantages are: (1) heat-losses without Fourier-components of the measuring frequency ω can be eliminated. (2) Quasi-isothermal determination of the heat capacity can be performed, not possible by standard DSC. (3) Reversible and irreversible heat-flow rate effects can be separated. (4) Heat capacity can safely be determined over a rather wide frequency range, even if steady state is not reached. The last point is of particular importance when the thermal event includes an irreversible latent heat. The extraction of the true heat capacity from the apparent heat capacity assures correct quantitative values when both measurements are properly deconvoluted and corrected. A note of caution is that large latent heats frequently destroy the steady state and

approach to steady state and need special attention [9]. The widely used adjustment of the measured frequency-dependent heat capacity in a temperature range outside of the transition region is the easiest way to get quantitative heat capacities within a transition region. However, this only works when data with sufficient high accuracy, as from the ATHAS data bank [20], are known. Otherwise, the more time-consuming procedure described in this paper could be used.

5. Conclusions

The power-compensated, temperature-modulated DSC with a sawtooth modulation of the program temperature can be used to determine the reversing heat capacity by fitting the true heat-flow rate and heating-rate amplitudes by the corresponding amplitudes of the first harmonics of the Fourier fit. Proper corrections must be applied, however, and are not available in the software that accompanied the TMDSC. The corrections are necessary to compensate the different approaches to steady state of the heat-flow rate and the heating rate when switching from one segment of the sawtooth to the next. Without these corrections, the results are distinctly frequency-dependent up to at least 100 s. The correction requires the evaluation of an instrument- and sample-dependent time constant. This time constant can be determined by the measurement of the frequency-dependence of the uncorrected heat capacity. Once the constant is known, measurements can be performed over practically the entire frequency range of the instrument, independent whether steady state is reached or not. The investigation shows that the data-treatment is different for power-compensation and heat-flux instruments.

Acknowledgements

This work was supported by the Division of Materials Research, National Science Foundation, Polymers Program, Grant No. DMR-9703692 and the Division of Materials Sciences, Office of Basic Energy Sciences, US Department of Energy at Oak Ridge National Laboratory, managed by Lockheed Martin Energy Research Corp. for the US Department of Energy, under Contract No. DE-AC05-96OR22464.

References

[1] A. Mehta, R.C. Bopp, U. Gaur, B. Wunderlich, J. Thermal Anal. 13 (1978) 197.
[2] B. Wunderlich, Thermal Analysis, Academic Press, New York, 1990.
[3] T.M.V.R. de Barros, R.C. Santos, A.C. Fernandes, M.E.M. da Piedade, Thermochim. Acta 269/270 (1995) 51.
[4] A. Boller, Y. Jin, B. Wunderlich, J. Therm. Anal. 42 (1994) 307.
[5] B. Wunderlich, Y. Jin, A. Boller, Thermochim. Acta 238 (1994) 277.
[6] B. Wunderlich, A. Boller, I. Okazaki, S. Kreitmeier, Thermochim. Acta 282/283 (1996) 143.
[7] B. Wunderlich, I. Okazaki, J. Thermal Anal. 49 (1997) 57.
[8] L.C. Thomas, A. Boller, I. Okazaki, B. Wunderlich, Thermochim. Acta 291 (1997) 85.
[9] B. Wunderlich, A. Boller, I. Okazaki, K. Ishikiriyama, W. Chen, M. Pyda, J. Pak, I. Moon, R. Androsch, Thermochim. Acta 330 (1999) 21.
[10] M. Reading, Trends Polym. Sci. 8 (1993) 248.
[11] M. Reading, A. Luget, R. Wilson, Thermochim. Acta 138 (1994) 295.
[12] B.G. Sumpter, D.W. Noid, G.L. Liang, B. Wunderlich, Adv. Polym. Sci. 116 (1994) 27.
[13] I. Moon, R. Androsch, B. Wunderlich, in: K.R. Williams (Ed.), Proceedings of the 26th NATAS Conference in Cleveland, OH, 13–15 September 1998, 26, 134.
[14] B. Schenker, F. Säger, Thermochim. Acta 304/305 (1997) 219.
[15] B. Wunderlich, in: K.R. Williams (Ed.), in: Proceedings of the 26th NATAS Conference in Cleveland, OH, 13–15 September 1998, 26, 140.
[16] G.W.H. Höhne, N.B. Shenogina, Thermochim. Acta 310 (1998) 47.
[17] J.E.K. Schawe, W. Winter, Thermochim. Acta 298 (1997) 9.
[18] Operating Instructions, Dynamic Differential Scanning Calorimetry (DDSC) Accessory Kit, Perkin–Elmer, Norwalk, 1995.
[19] R.B. Cassel, J.E.K. Schawe, Private Communication at the 26th NATAS Conference in Cleveland, OH, 13–15 September, 1998.
[20] Advanced Thermal Analysis System; B. Wunderlich, Pure and Applied Chem. 67, 1995, 1919. For downloadable data use WWW (Internet) URL: http://web.utk.edu/~athas/databank/vinyl/ps/ps.html
[21] F.U. Buehler, C.J. Martin, J.C. Seferis, J. Thermal Anal. 54 (1998) 501.
[22] R. Androsch, Additional, unpublished data.
[23] J.E.K. Schawe, Thermochim. Acta 271 (1996) 127.
[24] G.W.H. Höhne, E. Glöggler, Thermochim. Acta 151 (1989) 295.
[25] G.W.H. Höhne, J.E.K. Schawe, Thermochim. Acta 229 (1993) 27.
[26] A. Toda, T. Oda, M. Hikosaka, Y. Saruyama, Thermochim. Acta 293 (1997) 47.